Chinese Chemical Letters 37 (2026) 112640

Contents lists available at ScienceDirect

Chinese Chemical Letters

journal homepage: www.elsevier.com/locate/cclet

Fluorine-containing drugs approved by the FDA in 2025

Qian Wang[a], Yeping Bian[b,*], Elias Abouchabaka[c], Daniel Baecker[c,*], Gagan Dhawan[d,e,*], Anas Semghouli[f], Loránd Kiss[f,*], Wei Zhang[g,*], Vadim A. Soloshonok[h,*], Jianlin Han[a,*]

[a] *Jiangsu Co-Innovation Center of Efficient Processing and Utilization of Forest Resources, College of Chemical Engineering, Nanjing Forestry University, Nanjing 210037, China*
[b] *Department of Intensive Care Unit, Geriatric Hospital of Nanjing Medical University, Nanjing 210024, China*
[c] *Department of Pharmaceutical and Medicinal Chemistry, Institute of Pharmacy, Freie Universität Berlin, Königin-Luise-Straße 2+4, Berlin 14195, Germany*
[d] *School of Allied Medical Sciences, Delhi Skill and Entrepreneurship University, Dwarka, New Delhi 110077, India*
[e] *Department of Biomedical Science, Acharya Narendra Dev College, University of Delhi, Kalkaji, New Delhi 110019, India*
[f] *Institute of Organic Chemistry, Stereochemistry Research Group, HUN-REN Research Centre for Natural Sciences, Magyar tudósok krt. 2, Budapest H-1117, Hungary*
[g] *Department of Chemistry, University of Massachusetts Boston, Boston, MA 02125, United States*
[h] *IKERBASQUE, Basque Foundation for Science, María Díaz de Haro 3, Bilbao, Plaza Bizkaia 48013, Spain*

ARTICLE INFO

Article history:
Received 25 December 2025
Revised 9 March 2026
Accepted 17 March 2026
Available online 20 March 2026

Keywords:
Fluorine-containing compounds
Blockbuster drugs
Pharmaceuticals
Anti-cancer
Drug design and development
FDA
Asymmetric synthesis

ABSTRACT

Fluorine substitution has emerged as a cornerstone of modern drug design, profoundly influencing the pharmacological properties of therapeutic agents. Owing to its high electronegativity and small atomic radius, fluorine imparts unique electronic and steric effects that enhance lipophilicity, metabolic stability, binding affinity, and pK_a, thereby improving efficacy, bioavailability, and pharmacokinetics. Often referred to as an "enchanted atom", fluorine can decisively alter the trajectory of drug candidates, reducing attrition and increasing clinical success. Within synthetic organic chemistry, the pursuit of novel biologically active compounds is closely tied to monitoring advances in approved pharmaceuticals, with fluorine-containing drugs representing one of the most dynamic areas of innovation. In this review, we profile fourteen new pharmaceuticals approved by the U.S. Food and Drug Administration (FDA) in 2025, including datopotamab deruxtecan, suzetrigine, mirdametinib, avutometinib/defactinib, taletrectinib, sunvozertinib, sebetralstat, rilzabrutinib, imlunestrant, paltusotine, remibrutinib, elinzanetant, ziftomenib, and zoliflodacin. For each compound, we examine the medicinal chemistry discovery, therapeutic application, and FDA approval timeline, with particular emphasis on synthetic strategies and the role of fluorine incorporation. This review aims to provide a timely resource and inspiration for researchers in academia and the pharmaceutical industry, as well as for students engaged in drug design, fluorine chemistry, and medicinal chemistry.

© 2026 Published by Elsevier B.V. on behalf of Chinese Chemical Society and Institute of Materia Medica, Chinese Academy of Medical Sciences.

1. Introduction

Fluorine substitution is a cornerstone of modern drug design because it can dramatically enhance the pharmacological profile of a molecule. Fluorine, with its high electronegativity and small atomic radius, exerts unique electronic and steric effects when introduced into drug candidates. This substitution often improves lipophilicity, metabolic stability, binding affinity, and pK_a, which in turn enhances therapeutic efficacy, bioavailability, and pharmacokinetics. Medicinal chemists frequently refer to fluorine as an "enchanted atom" because even a single fluorine atom can reshape the fate of a drug candidate, reducing failure rates and increasing the likelihood of clinical success. By fine-tuning molecular interactions with biological targets and slowing metabolic degradation, fluorine substitution has become a strategic tool for optimizing lead compounds and ensuring that promising molecules reach the market [1–7]. On the other hand, fluorine plays a unique role in influencing molecular conformation. Its impact extends far beyond simple steric bulk, encompassing a multidimensional influence that integrates spatial, electronic, and conformational dynamics. The van der Waals radius of fluorine (~1.47 Å) is close to that of hydrogen (~1.20 Å), which allows fluorine substitution to often maintain the overall molecular shape. However, as the most electronegative element (3.98, Pauling scale), fluorine strongly polarizes bonds and

* Corresponding authors.
E-mail addresses: bianyeping@jspgh.com (Y. Bian), d.baecker@fu-berlin.de (D. Baecker), gagandhawan@andc.du.ac.in (G. Dhawan), kiss.lorand@ttk.hu (L. Kiss), wei2.zhang@umb.edu (W. Zhang), vadym.soloshonok@ehu.es (V.A. Soloshonok), hanjl@njfu.edu.cn (J. Han).

https://doi.org/10.1016/j.cclet.2026.112640
1001-8417/© 2026 Published by Elsevier B.V. on behalf of Chinese Chemical Society and Institute of Materia Medica, Chinese Academy of Medical Sciences.

alters local electron density. These properties make fluorine a key mediator of polar steric effects. In aliphatic scaffolds, fluorine often adopts a stable gauche relationship with adjacent polar bonds, which can preorganize pharmacophores into bioactive orientations. Moreover, when fluorine atom is directly attached to a chiral carbon, its high electronegativity can electronically perturb neighboring groups, creating a unique chiral environment [8].

One of the central aims of synthetic organic chemistry is the creation of novel biologically active compounds, and researchers therefore monitor advances in approved pharmaceuticals with great attention. In this context, comprehensive review articles are welcomed with particular enthusiasm, as they provide critical insights into emerging trends. Among these, the field of fluorine-containing drugs stands out for its exceptional dynamism. The strategic incorporation of fluorine atoms has repeatedly proven to transform pharmacological properties, influencing potency, selectivity, metabolic stability, and bioavailability. As a result, annual updates in this area are eagerly anticipated, reflecting both the rapid pace of innovation and the profound impact of fluorine substitution on modern drug development [9–15].

In this review, we highlight fourteen novel fluorine-containing pharmaceuticals that received approval from the U.S. Food and Drug Administration (FDA) for market entry in 2025. These agents include datopotamab deruxtecan (Datroway) (**1**), suzetrigine (Journavx) (**2**), mirdametinib (Gomekli) (**3**), the combination therapy of avutometinib and defactinib (Avmapki) (**4**), taletrectinib (Ibtrozi) (**5**), sunvozertinib (Zegfrovy) (**6**), sebetralstat (Ekterly) (**7**), rilzabrutinib (Wayrilz) (**8**), imlunestrant (Inluriyo) (**9**), paltusotine (Palsonify) (**10**), remibrutinib (Rhapsido) (**11**), elinzanetant (Lynkuet) (**12**), ziftomenib (Komzifti) (**13**), and zoliflodacin (Nuzolvence) (**14**). The chemical structures of these newly approved drugs are depicted in Fig. 1, providing a visual overview of their molecular diversity and design.

For each compound, this review examines the path of medicinal chemistry discovery, the therapeutic area addressed, and the timeline leading to FDA approval. Special emphasis is placed on the detailed step-by-step synthetic strategies, with particular focus on the introduction of fluorine and its impact on molecular design. We anticipate that this review will serve as a valuable resource and source of inspiration for practitioners in academia and the pharmaceutical industry, as well as for students engaged in drug design, fluorine chemistry, and medicinal chemistry more broadly.

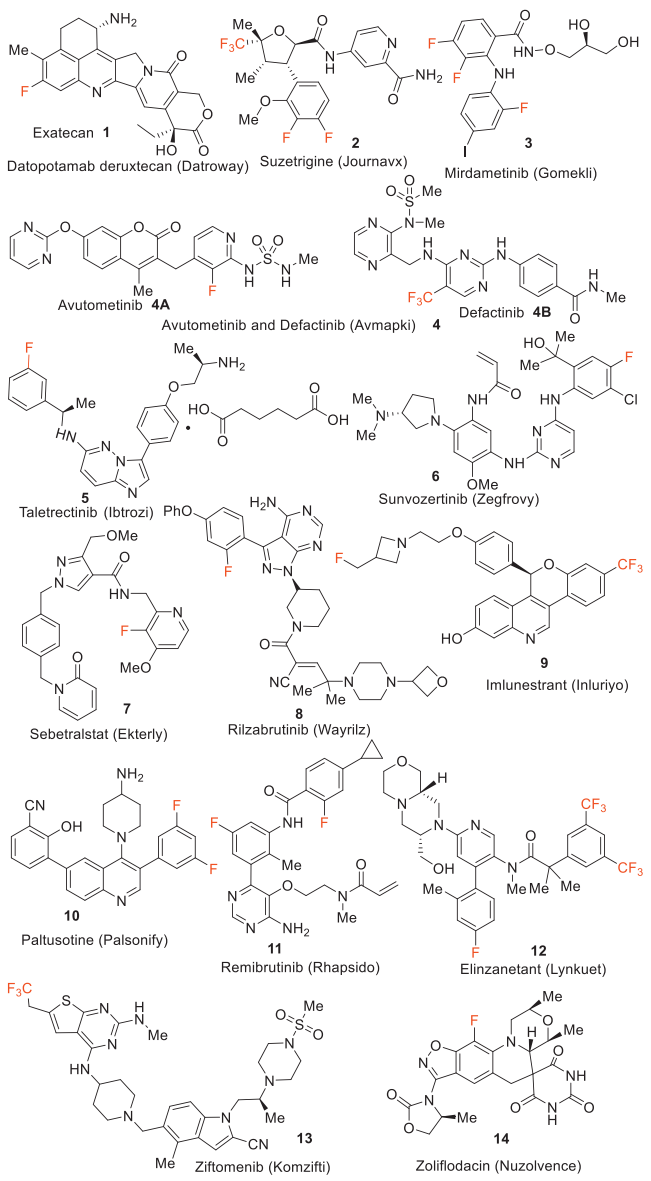


Fig. 1. Structures of fourteen novel fluorine-containing pharmaceuticals that received approval from the FDA for market entry in 2025.

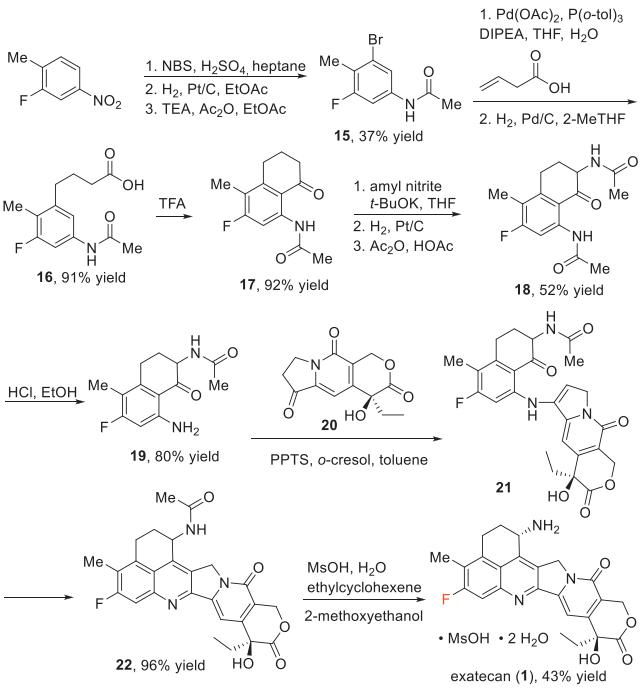
2. Datopotamab deruxtecan (Datroway)

Datopotamab deruxtecan (brand name: Datroway) represents an antibody drug conjugate. The monoclonal antibody targets the trophoblast cell surface antigen 2 (TROP2). The latter is expressed in various tumors, with overexpression occurring particularly in hormone receptor (HR)-positive and human epidermal growth factor receptor 2 (HER2)-negative breast cancer. The FDA approved datopotamab deruxtecan on January 17, 2025, for treating patients who have an unresectable or metastatic form of this type of breast cancer (HR+, HER2-) after getting endocrine-based therapy and chemotherapy for unresectable or metastatic disease before [16].

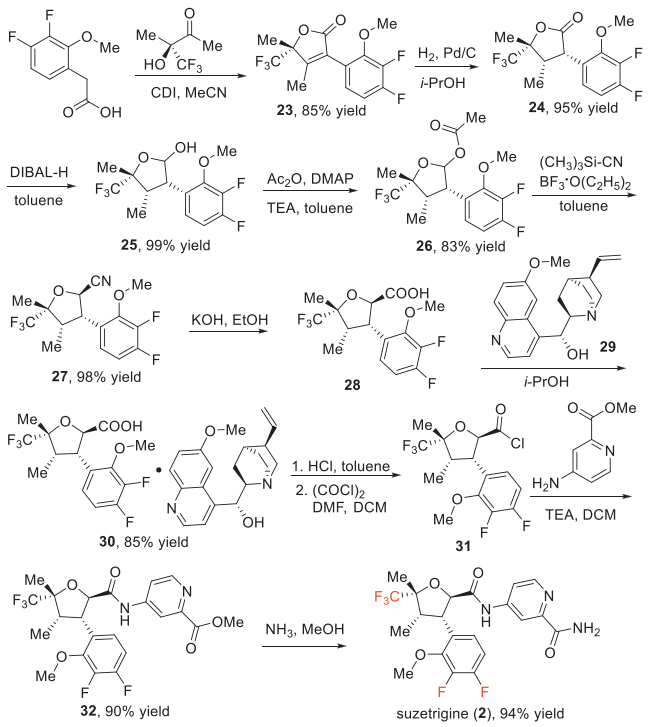
The antibody datopotamab is bound to deruxtecan. A thiol group of the antibody is used to form a covalent thioether bond with the maleimide group of deruxtecan in the manner of a Michael addition [17]. Structurally, deruxtecan comprises a maleimidocaproamide spacer, a cleavable tetrapeptide-based linker (G-G-F-G), and the topoisomerase I (TOP1) inhibitor exatecan [18].

Exatecan (**1**) is a structural analog of the alkaloid camptothecin, whereby exatecan exhibits a striking fluorination. For camptothecin-derived TOP1 inhibitors, improved metabolic activity was observed as a result of introducing fluorine [19,20]. Fluorination at the A-ring of the pyranoindolizino-quinoline-based core leading to fluorocamptothecins caused, for example, increased cytotoxicity *in vitro* and *in vivo* and reduced systemic toxicity in mice compared to camptothecin [21].

Exatecan (**1**), the actual fluorine-containing constituent of datopotamab deruxtecan, could be synthesized as follows (Scheme 1). The synthesis started with 2-fluoro-1-methyl-4-nitrobenzene, which was brominated using *N*-bromosuccinimide (NBS) and sulfuric acid in heptane, followed by platinum-catalyzed hydrogenation reduction of the nitro substituent in ethyl acetate (EtOAc) to give the respective aniline. The latter was then acetylated with acetic anhydride (Ac_2O) in the presence of triethylamine (TEA) in EtOAc to yield the brominated anilide **15**. This aryl bromide **15** was subject to a palladium-catalyzed C–C coupling reaction with but–3-enoic acid in the presence of *N*,*N*-diisopropylethylamine (DIPEA) to an alkene intermediate, which was then hydrogenated in 2-methyle-tetrahydrofurane (2-MeTHF) to give the acid **16**. The carboxylic acid was activated with trifluoroacetic acid (TFA) to react in a kind of intramolecular Friedel-Crafts acylation resulting in the tetrahydronaphthalenone



Scheme 1. Synthesis of exatecan (**1**).



Scheme 2. Synthesis of suzetrigine (**2**).

derivative **17**. Then, amyl nitrite and potassium *tert*–butanolate (*t*-BuOK) in tetrahydrofuran (THF) were used to nitrate in the α-position to the ketone, followed by catalytic hydrogenation of the nitro group to form a primary amine. This was finally converted to compound **18** with Ac_2O in acetic acid (HOAc). Deacetylation of the anilide, selective compared to the carboxylic acid amide of the aliphatic primary amine, was achieved with hot hydrochloric acid in ethanol (EtOH) and yielded the amine **19**. This was followed by a reaction with ketone **20**, the synthesis of which was also reported in the literature [22]. In 2-hydroxytoluene (*o*-cresol) and toluene as solvents, the primary aromatic amine **19** reacted with the ketone group of **20** in the presence of pyridinium *p*-toluenesulfonate (PPTS) to form the enamine **21** in a condensation reaction. This enamine **21** cyclized in a dehydrative manner to the quinoline **22**. Since this was obtained as a mixture of diastereomers, it was necessary to perform the most stereoselective possible cleavage of the secondary amide to the primary amine of exatecan (**1**). This was done, for example, in ethylcyclohexene and 2-methoxyethanol with aqueous methanesulfonic acid (MsOH). This produced the mesylate amine salt dihydrate of exatecan (**1**) on the one hand and the diastereomer *epi*–exatecan on the other, which was separated off and underwent an amine reprotection-deprotection-crystallization sequence [23].

3. Suzetrigine (Journavx)

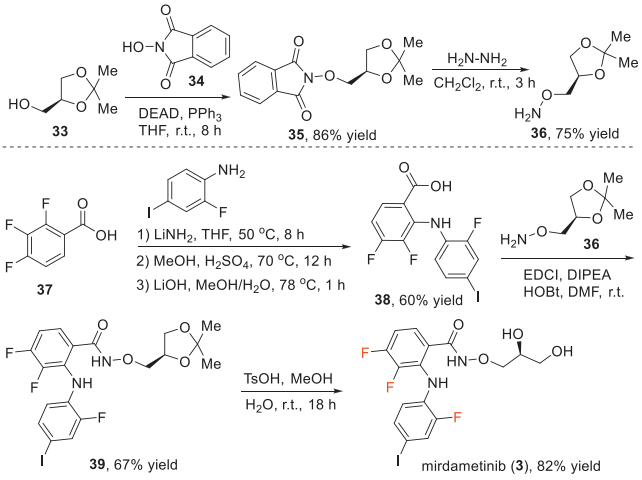
Suzetrigine (**2**, brand name: Journavx) has been approved by the FDA on January 30, 2025 for the treatment of moderate to severe acute pain. The mode of action is based on the inhibition of the voltage-gated sodium channel $Na_V1.8$. The inhibition is selective relative to other Na_V channel subtypes [24]. Since suzetrigine (**2**) is a non-opioid analgesic, the drawbacks of opioids, such as severe side effects, occurrence of tolerance, and dependence, can be better circumvented. Suzetrigine can be considered as an innovation because it is the first approved Na_V inhibitor for pain therapy [25].

Structurally, suzetrigine (**2**) is a pyridine derivative that also has an oxolane core (tetrahydrofuran). The latter contains four stereogenic centers of the drug molecule as well as substitution with trifluoromethyl and a 3,4-difluoro-2-methoxyphenyl ring [26]. With regard to the structure-activity relationship (SAR), taking into account other developed $Na_V1.8$ inhibitors, an aryl-linked amide and fluorination can be identified [27]. Given the hydrophobicity of the fluorine substituents, the binding of the drug to a hydrophobic chasm within the target is supported and metabolic stability is increased [28].

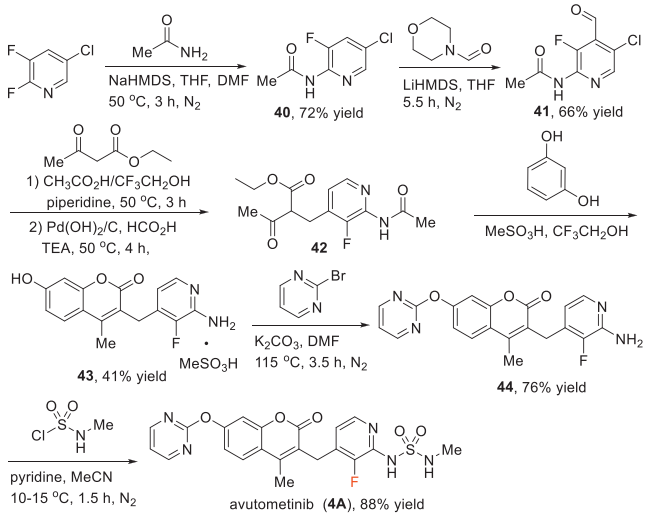
The synthetic route (Scheme 2) to obtain suzetrigine (**2**) began with 2-(3,4-difluoro-2-methoxyphenyl)acetic acid. It was activated using 1,1′-carbonyldiimidazole (CDI) in acetonitrile and then treated with (*S*)-4,4,4-trifluoro-3–hydroxy–3-methylbutan-2-one, subsequently giving the unsaturated γ-lactone **23**. The α,β-double bond of the lacton **23** was hydrogenated to the saturated γ-lactone **24** using 5% palladium on carbon in isopropyl alcohol (*i*-PrOH) as a catalyst. The lactone **24** was further reduced employing diisobutylaluminium hydride (DIBAL-H) in toluene to afford the hemiacetal **25**. The latter was acetylated to compound **26** with Ac_2O in toluene using 4-dimethylaminopyridine (DMAP) and TEA. The obtained ester **26** was reacted with trimethylsilyl cyanide in the presence of boron trifluoride etherate to yield the nitrile **27**. Hydrolysis with potassium hydroxide in EtOH converted the nitrile **27** into the carboxylic acid **28**. With the aid of quinine **29** in *i*-PrOH, acid **28** formed the salt **30** in order to allow for enantiomeric resolution. To release the free acid, the obtained salt **30** was first treated with aqueous hydrochloric acid in toluene, followed by activation using oxalyl chloride in *N,N*-dimethylformamide (DMF) to give the acid chloride **31**. Formation of the secondary amide **32** was accomplished in the presence of TEA using methyl 4-aminopicolinate. Transformation of the methyl ester to a primary amide by reaction of **32** with ammonia solution in methanol eventually resulted in suzetrigine (**2**) [29].

4. Mirdametinib (Gomekli)

Mirdametinib (**3**, brand name: Gomekli) acts by inhibiting the mitogen-activated protein kinase kinases 1 and 2 (MEK1/2), thus



Scheme 3. Synthesis of mirdametinib (**3**).



Scheme 4. Synthesis of avutometinib (**4A**).

interfering with the Ras-Raf-MEK1/2-ERK pathway. It was approved by the FDA on February 11, 2025 for the treatment of neurofibromatosis type 1 (NF1) in both adults and children (aged 2 and above) having symptomatic plexiform neurofibromas, *i.e.*, noncancerous tumors of the peripheral nerve sheath, which are not suitable for complete resection [30].

The drug represents a derivative of benzohydroxamic acid esterified with glycerol. Its phenyl ring is part of a diphenylamine skeleton, being substituted twice with fluorine, while the other ring bears one fluorine substituent [31]. In the context of fluorine scanning, it was generally found that fluorination can enhance the Raf/MEK inhibition [32]. Reviewing structural features of several MEK inhibitors revealed that fluorinated compounds showed the highest potency against MEK [33,34]. In particular, fluorine substituents of both phenyl rings of the diarylamine core in the structure of mirdametinib contribute to the interaction in the binding pocket of MEK1 *via* Lys97 and Ser212 [35].

The preparation of mirdametinib (**3**) can be performed following a convergent synthesis (Scheme 3). For this approach, the *S*-configured glycerol acetonide **33** was coupled with *N*-hydroxyphthalimide (**34**) in the presence of diethyl azodicarboxylate (DEAD) and PPh_3 to give the isoindole-1,3–dione derivative **35** in 86% yield. The subsequent hydrazinolysis provided the *O*-substituted hydroxylamine intermediate **36**.

The reaction of 2-fluoro-4-iodoaniline and 2,3,4-trifluorobenzoic acid (**37**) in the presence of the base lithium amide followed by esterification and hydrolysis led to the diphenylamine **38**. Next, the benzoic acid derivative **38** was coupled with the hydroxylamine **36** in the presence of 1-(3-dimethylaminopropyl)-3-ethylcarbodiimide hydrochloride/1-hydroxybenzotriazole (EDCI/HOBt) to give the carbamate **39** in 67% yield. The final deprotection of the ketal to give the diol resulted in mirdametinib (**3**) in 82% yield [36].

5. Avutometinib and defactinib (Avmapki)

Avutometinib (**4A**) and defactinib (**4B**) are two inhibitors of different kinases, co-packaged (brand name: Avmapki Fakzynja Co-Pack) for the treatment of patients suffering from KRAS-mutated recurrent low-grade serious ovarian cancer (LGSOC) who have already received systemic therapy before. Approval by the FDA was granted in May 2025 [37].

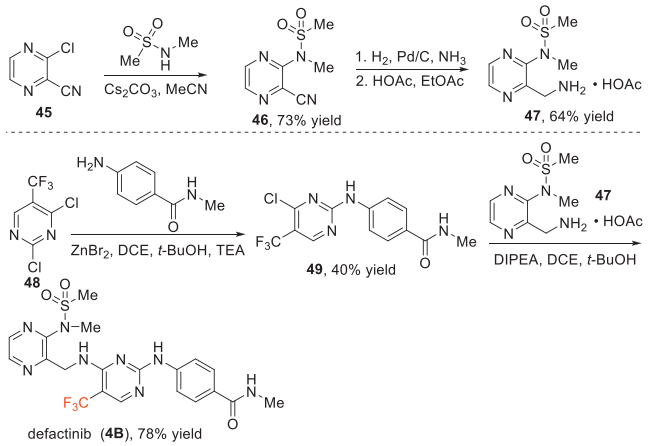
In particular, avutometinib (**4A**) also interferes with the Ras-Raf-MEK-ERK signaling pathway, but in a distinct manner by inhibiting both Raf and MEK kinases. Based on this dual acting, avutometinib inhibits the MAPK pathway more efficiently than a conventional MEK inhibitor [38]. Structurally, avutometinib (**4A**) has a 4-methylchromen-2-one scaffold, which is pyrimidine-2-yloxy-substituted and also carries a pyridin-4-ylmethyl substituent. The latter is methylsulfamoylamino-substituted in position 2 and fluorinated in position 3. The fluorine substituent at the pyridine increases the metabolic stability and contributes to the lipophilicity of the drug [39].

The synthesis of avutometinib (**4A**) (Scheme 4) started from nucleophilic substitution of 5–chloro–2,3-difluoropyridine by acetamide in the presence of sodium hexamethyldisilazide (NaHMDS) leading to the intermediate **40** in 72% yield. Then, formylation of the intermediate **40** using morpholine-4-carbaldehyde in the presence of lithium hexamethyldisilazide (LiHMDS) generated aldehyde **41**, which underwent condensation reaction with ethyl 3-oxobutanoate followed by reduction yielding the intermediate **42**. Further reaction with resorcinol under acidic conditions yielded the 7-hydroxylated coumarin derivative **43** in a Pechmann condensation. The phenol **43** was deprotonated using potassium carbonate, followed by a reaction with 2-bromopyrimidine in THF to give the phenolic ether **44** in 76% yield. Finally, reaction with methylsulfamoyl chloride in MeCN and coexistence of a base such as pyridine afforded avutometinib (**4A**) [40].

Defactinib (**4B**) is an inhibitor of the non-receptor tyrosine kinase, focal adhesion kinase (FAK) [41]. In addition, the proline-rich tyrosine kinase-2 (Pyk2) is inhibited by defactinib (**4B**), too. Chemically, defactinib (**4B**) consists of a 2,4-diaminopyrimidine core, which is widely discussed as a structural feature of FAK inhibitors [42–44]. However, the pyrimidine ring also carries a trifluoromethyl substituent in position 5 in the structure of defactinib. This fluorine-containing substituent forms a halogen bond with Asp564 in a hydrophobic site of FAK, thus contributing to the binding [45]. The fluorination improves affinity and metabolic stability [39].

To prepare defactinib (**4B**) in a convergent synthetic strategy (Scheme 5), 2-chloropyrazine (**45**) was reacted in MeCN with *N*-methylmethanesulfonamide, which was deprotonated using cesium carbonate, to obtain the aromatic sulfonamide **46** in 73% yield. Next, reduction of the nitrile to the (aminomethyl)pyrazine **47** was achieved with catalytic hydrogenation in methanolic ammonia, followed by treatment with HOAc in EtOAc.

The 5-trifluoromethyl-substituted pyrimidine derivative **48** was converted to the diarylamine intermediate **49** with 4-amino-*N*-methylbenzamide using zinc(II) bromide and TEA in dichloroethane (DCE) and *tert*–butanol (*t*-BuOH). Finally, (aminomethyl)pyrazine



Scheme 5. Synthesis of defactinib (**4B**).

47 and diarylamine **49** were coupled within a nucleophilic substitution again in DCE and *t*-BuOH with DIPEA serving as a non-nucleophilic base to result in defactinib (**4B**) in 78 % yield [46].

6. Taletrectinib (Ibtrozi)

Taletrectinib (**5**, brand name: Ibtrozi) is an oral medication originally discovered by Daiichi Sankyo and developed by Nuvation Bio Inc. for treating adults with locally advanced or metastatic, ROS1-positive NSCLC [47–49]. It is a potent and selective inhibitor that primarily targets the ROS1 tyrosine kinase. The drug is specifically designed to treat tumors driven by ROS1 gene fusions. Its mechanism of action involves selectively blocking the ROS1 receptor tyrosine kinase. This blockade effectively disrupts the downstream signaling cascades that cancer cells depend on for their growth and survival. By inhibiting these pathways, taletrectinib (**5**) reduces the proliferation of ROS1-positive tumor cells. The drug also exhibits activity against the related neurotrophic tyrosine receptor kinase (NTRK) family of kinases (TRKA/B/C) and it has shown effectiveness against certain ROS1 resistance mutations that can emerge after earlier lines of therapy [50–52]. SAR studies revealed that the fluorine substituent on the phenyl ring shows an important role in the ROS1 kinase inhibitory activity (Fig. 2). For example, compound **51** with a fluorine atom showed a high inhibitory activity with <20 nmol/L ROS1 IC_{50} value. A decreased inhibitory activity was observed for the compound **50** without fluorine substituent [53]. On June 11, 2025, taletrectinib (**5**) received FDA approval for treating adult patients with locally advanced or metastatic, ROS1-positive NSCLC [54].

The synthesis of taletrectinib (**5**) was illustrated in Scheme 6. It commenced with the reaction of (*R*)-1-(3-fluorophenyl)ethan-1-amine with 3–bromo–6-chloroimidazo[1,2-*b*]pyridazine in dimethyl sulfoxide (DMSO) to afford (*R*)-3–bromo–*N*-(1-(3-fluorophenyl)ethyl)imidazo[1,2-*b*]pyridazin-6-amine. Then, this aryl bromide underwent a Suzuki coupling reaction with boronic

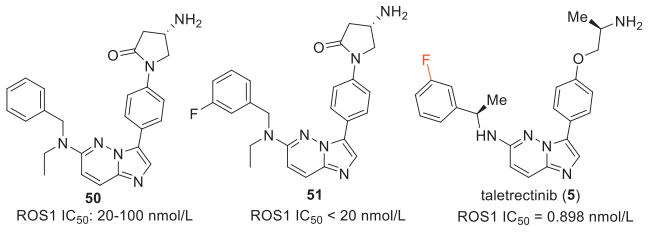
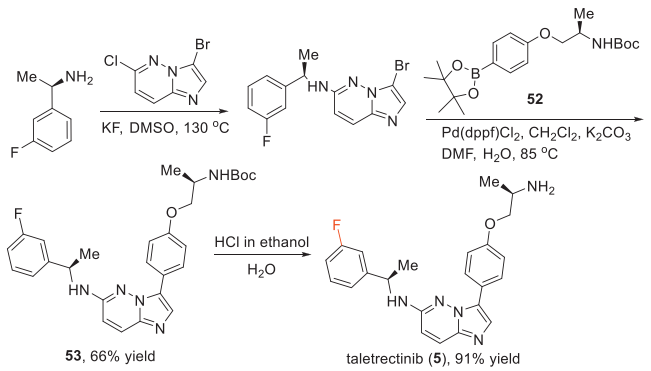


Fig. 2. SAR optimization for taletrectinib (**5**).



Scheme 6. Synthesis of taletrectinib (**5**).

acid **52**, affording Boc-protected amine **53** in 66 % yield. Sequential acidolysis/deprotection of Boc-protected amine **53** led to the formation of taletrectinib (**5**) in 91 % yield [55,56].

7. Sunvozertinib (Zegfrovy)

Sunvozertinib (**6**, brand name: Zegfrovy) is an oral, covalent epidermal growth factor receptor (EGFR) tyrosine kinase inhibitor (TKI) developed by Dizal (Jiangsu) Pharmaceuticals for the treatment of NSCLC. In July 2025, the FDA granted accelerated approval to sunvozertinib (**6**) for adults with locally advanced or metastatic NSCLC carrying EGFR exon 20 insertion mutations whose disease has progressed following platinum-based chemotherapy. Preclinical studies, including work in cell lines and xenograft models, have shown that sunvozertinib (**6**) has strong antitumor activity. Sunvozertinib (**6**) displays strong inhibitory activity against a broad range of EGFR exon20ins variants while exerting comparatively limited effects on wild-type EGFR, an attribute intended to reduce dose-limiting toxicity. Mechanistically, the drug forms an irreversible covalent bond within the ATP-binding pocket of the EGFR kinase domain, thereby blocking downstream signaling pathways that drive tumor cell proliferation and survival [57–72]. Fluorine contributes a surface that is largely hydrophobic in shape yet still carries distinct electronic features, allowing the molecule to fit more effectively into hydrophobic pockets within EGFR. The SAR studies showed high inhibitory activity with IC_{50} values against pEGFR T790M of 0.32, 0.3, and 1.1 nmol/L for compounds **54**, **55**, and sunvozertinib (**6**), respectively. Notably, introducing both 4-fluoro and 5–chloro substitutions into compound **54** successfully reduced human hepatocyte clearance from 34 (μL/min)/(10^6 cells) to 7.1 (μL/min)/(10^6 cells) (Fig. 3) [73].

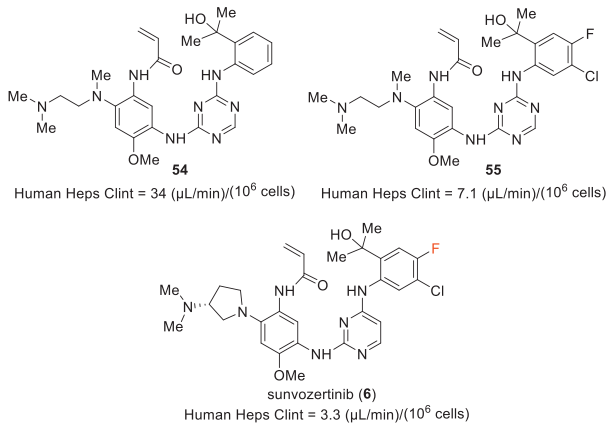
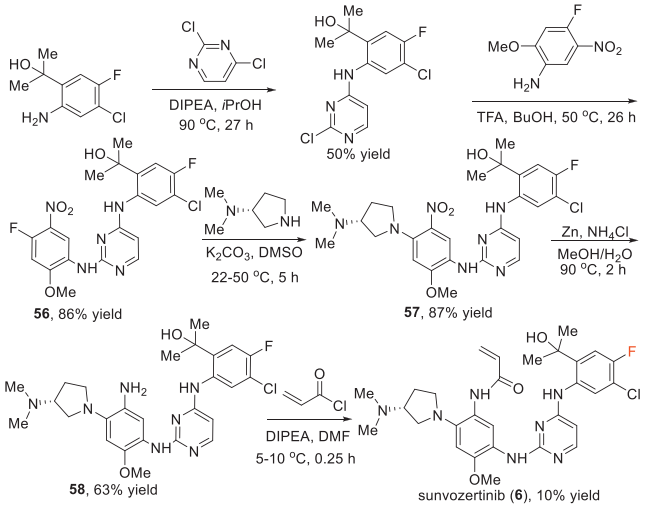


Fig. 3. SAR optimization for sunvozertinib (**6**).



Scheme 7. Synthesis of sunvozertinib (**6**).

The synthesis of sunvozertinib (**6**) was shown in Scheme 7 [73–75]. Substitution reaction between 2-(2-amino-4–chloro–5-fluorophenyl)propan-2-ol and 2,4-dichloropyrimidine with DIPEA as a base generated the intermediate in 50% yield, which underwent another substitution reaction by 4-fluoro-2–methoxy–5-nitroaniline affording the intermediate **56** in 86% yield. Subsequently, treatment of intermediate **56** with (*R*)-*N,N*-dimethylpyrrolidin-3-amine in the presence of K_2CO_3 yielded the nitro compound **57** in 87% yield. A reductive transformation of nitro compound **57** using zinc and NH_4Cl proceeded cleanly under heating to give the amine intermediate **58** in 63% yield. In the final synthetic step, reaction of amine **58** with acryloyl chloride in the presence of DIPEA afforded the desired sunvozertinib (**6**) in 10.5% yield.

8. Sebetralstat (Ekterly)

There are several orally available small-molecule protein kinase A (PKa) inhibitors that have entered clinical trials [76–82], such as avoralstat [83], berotralstat [84], ATN-249 [85,86], and sebetralstat (**7**). Among them, sebetralstat (**7**, brand name: Ekterly) developed by Kalvista Pharmaceuticals was approved by the FDA in July 2025 for the treatment of hereditary angioedema (HAE). By inhibiting plasma kallikrein, it prevents the excessive generation of bradykinin and thereby helps to stop or diminish the development of a swelling episode. HAE attacks stem from the overactivation of the kallikrein–kinin system, which increases vascular permeability and leads to fluid leakage into tissues [87].

The SAR insights gained from the early plasma-kallikrein inhibitor series guided the development of the more potent scaffolds represented by compounds **59** and **60**, both featuring a benzylpyridone P4 moiety and a pyrazole amide core (Fig. 4). These findings prompted a re-examination of how ligands engage the P1 region, exploring binding modes that do not depend on the classical ionic interaction with Asp189. Compound **60** emerged as a suitable template for designing a series of phenyl-based P1 substituents. Subsequent lead-optimization steps produced compound **61**, which incorporated two key improvements: (i) Including modification of the pyrazole core to enhance membrane permeability, and (ii) introduction of a pyridine P1 group to reduce lipophilicity and increase aqueous solubility to form the structure of sebetralstat (**7**) [88]. Sebetralstat (**7**) contains a strategically positioned fluoro substituent. Fluorine can also contribute to productive hydrophobic interactions within the kallikrein binding pocket and can influence

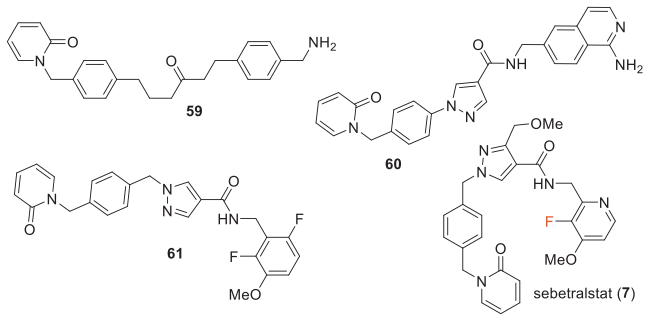
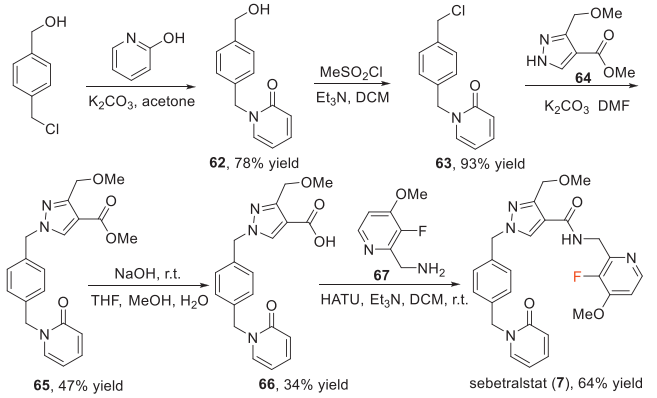


Fig. 4. SAR optimization for sebetralstat (**7**).



Scheme 8. Synthesis of sebetralstat (**7**).

the preferred molecular geometry through stereoelectronic effects such as the gauche effect. Together, these features help balance lipophilicity, permeability, and clearance, contributing to the favorable pharmacokinetic profile of sebetralstat (**7**).

The synthesis of sebetralstat (**7**) was shown in Scheme 8. The *N*-benzylpyridone alcohol intermediate **62** was prepared through a regioselective alkylation of 2-hydroxypyridine with a 4-(chloromethyl)benzyl alcohol. Functional group interconversion of alcohol **62** to 1-(4-chloromethyl-benzyl)-1*H*-pyridin-2-one **63** in 93% yield was achieved *via* the formation of methanesulfonate to afford a suitably activated electrophile for subsequent coupling steps. Intermediate **63** was reacted with a methoxymethyl-substituted pyrazole ester **64** under basic conditions affording intermediate **65** in 47% yield. Hydrolysis of the ester **65** yielded the corresponding carboxylic acid **66** in 34% yield, which was subsequently coupled with (3-fluoro-4-methoxypyridin-2-yl)methanamine (**67**) under general amination conditions to give the target sebetralstat (**7**) in 64% yield [88].

9. Rilzabrutinib (Wayrilz)

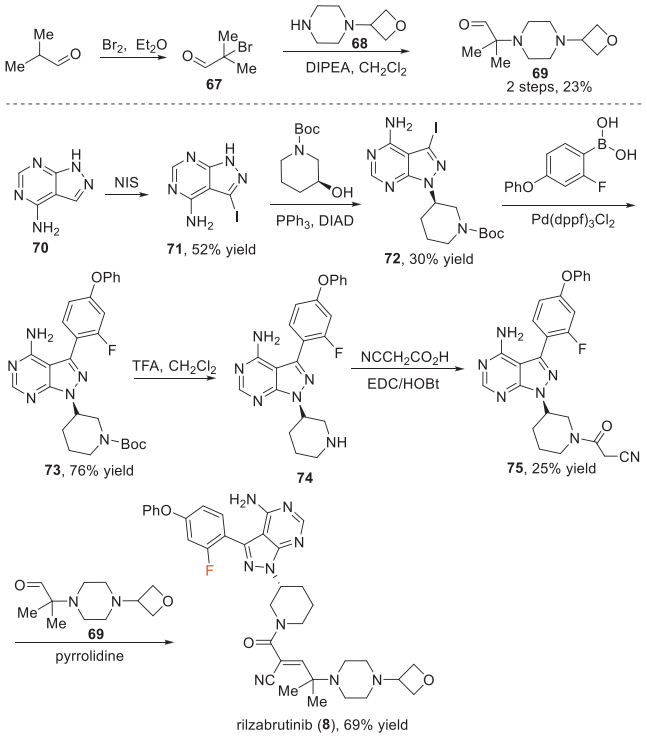
Rilzabrutinib (**8**, brand name: Wayrilz) is a product of the clear evolution from irreversible, cancer-focused Bruton's tyrosine kinase (BTK) inhibitors to reversible, more selective inhibitors for autoimmune diseases. Its "lead molecules" are both the pioneering ibrutinib [89–95] and the reversible predecessors like fenebrutinib [96] that validated the approach of targeting BTK without a covalent bond. The FDA approved drug developed by Sanofi, rilzabrutinib (**8**), on August 29, 2025, for adults with persistent or chronic immune thrombocytopenia (ITP). This treatment is specifically for patients who have already tried other therapies, such as immunoglobulins, anti-D therapy, and corticosteroids, without sufficient success. It is not intended as a first-line treatment. Rilzabrutinib (**8**) works by reversibly inhibiting a protein called BTK. This

action helps regulate the faulty attack on platelets by the immune system. For patients, this can lead to a relatively quick and lasting increase in platelet counts, as well as an improvement in other symptoms related to ITP.

Rilzabrutinib (**8**) tackles ITP in two keyways. First, it calms down the overactive B-cells of the immune system by blocking a key signal (BTK-mediated B-cell receptor signaling). This reduces the production of harmful "autoantibodies" that mistakenly tag the own platelets of the body for destruction. Second, it helps protect the platelets that are already in circulation. It does this by interfering with messages that tell immune cells called macrophages to "eat" the antibody-coated platelets, a process that primarily happens in the spleen and liver. Because it addresses this underlying immune misfiring, rilzabrutinib (**8**) is often described as an orphan drug that targets a root cause of ITP, rather than just boosting platelet production like other treatments (thrombopoietin receptor agonists) do [97,98].

The single fluorine atom in the chemical structure of rilzabrutinib is a key design feature that significantly enhances the efficacy of the drug. Rilzabrutinib (**8**) exhibited a high inhibitory activity against BTK with an IC_{50} value of 1.3 nmol/L. In the human whole blood (HWB) CD69 B-cell activation assay, it also demonstrated a trend toward high potency ($IC_{50} = 123 \pm 38$ nmol/L; $n = 8$). The early SAR studies disclosed that fluorine atom was a preferred substituent for the diaryl ether linkage, affording improved inhibition of CD69 expression on anti-IgM-stimulated B cells in HWB [99].

The synthesis of rilzabrutinib (**8**) was outlined in Scheme 9 [99,100]. The aldehyde **69** and nitrile **75** are the key intermediates which were made in a convergent synthesis. The aldehyde **69** was synthesized from isobutyraldehyde. Isobutyraldehyde was brominated to form 2–bromo–isobutyraldehyde **67**, which directly reacted with the 1-(oxetan-3-yl)piperazine (**68**) in the presence of DIPEA to provide aldehyde **69**. Another key cyanoamide intermediate **75** was obtained through a five-step linear sequence starting from iodination of 1*H*-pyrazolo[3,4-*d*]pyrimidin-4-amine



Scheme 9. Synthesis of rilzabrutinib (**8**).

(**70**) by using *N*-iodosuccinimide (NIS). Then, Mitsunobu reaction of the intermediate **71** with *tert*–butyl (*S*)-3-hydroxypiperidine-1-carboxylate in the presence of diisopropyl azodicarboxylate (DIAD) and PPh_3 afforded the intermediate **72**, which underwent Suzuki–Miyaura coupling with (2-fluoro-4-phenoxyphenyl)boronic acid yielding the intermediate **73** in 76% yield. Boc-deprotection followed by an amidation reaction with cyanoacetic acid using ethyldimethylaminopropyl carbodiimide (EDC)/HOBt as coupling agents gave the cyanoamide intermediate **75**. Final step for the construction of the targeted rilzabrutinib (**8**) was achieved through the Knoevenagel condensation between cyanoamide **75** and aldehyde **69** in 69% yield as a 9:1 *E/Z* mixture. The unwanted *Z* isomer was removed by purification *via* flash column chromatography to afford rilzabrutinib (**8**) in 29% yield.

10. Imlunestrant (Inluriyo)

Imlunestrant (**9**, brand name: Inluriyo) is a brain-penetrant selective estrogen receptor degrader (SERD) developed by Eli Lilly and Company (Indianapolis, IN, USA) to provide continuous inhibition of estrogen receptor (ER) α, including ESR1-mutant variants that increase endocrine resistance in ER-positive, HER2-negative advanced breast cancer [101,102]. On September 25, 2025, it received its first approval from the FDA for the treatment of ER+, HER2- estrogen receptor 1-mutated advanced or metastatic breast cancer with disease progression following at least one line of endocrine therapy [101–103]. Imlunestrant (**9**) binds to and degrades ERα with high potency ($K_i = 0.64$ nmol/L; DC_{50} < 1 nmol/L) and maintains strong affinity for the Y537S mutant ($K_i = 2.8$ nmol/L), outperforming non-trifluoromethylated analogs **76** ($K_i = 8.11$–27.23 nmol/L) as illustrated in Fig. 5, emphasizing the effect of strategic fluorine substitution on receptor engagement and metabolic stability [104]. Clinically, Imlunestrant (**9**) monotherapy achieves mPFS values of 5.5–7.2 months and shows superior efficacy in ESR1-mutated tumors, with a favorable safety profile dominated by low-grade gastrointestinal symptoms and fatigue [105]. With potent ER degradation, mutation-agnostic activity, and brain penetration, imlunestrant (**9**) represents a significant advancement in endocrine therapy and a strong backbone for future combination strategies [101–105].

The synthesis of imlunestrant (**9**) as outlined in Scheme 10 started with aldehyde **77**, which was treated with 4-fluorophenylmagnesium bromide in THF at −78 °C, followed by MnO_2-mediated oxidation under reflux in dichloromethane (DCM) to afford the ketone intermediate **78**. Subsequent demethylation with boron tribromide yielded the corresponding phenolic derivative **79**. This intermediate **79** then underwent a Mitsunobu reaction with 2-[3-(fluoromethyl)azetidin-1-yl]ethanol (**80**) to provide ether-linked product **81** in 61% yield. A palladium-catalyzed Suzuki–Miyaura coupling with (4-(trifluoromethyl)phenyl)boronic acid furnished the biaryl quinoline ketone **82**. Reduction of this ketone **82** with lithium triethylborohydride in 1,4-dioxane, followed by cyclization using NaH under reflux conditions, afforded racemic imlunestrant ((±)-**9**). Finally, chiral supercritical fluid

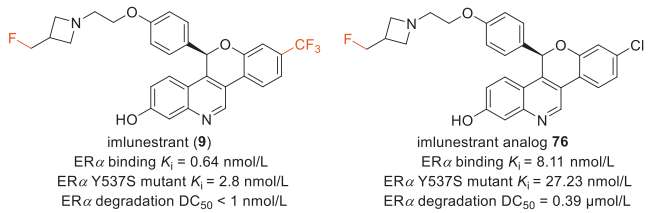
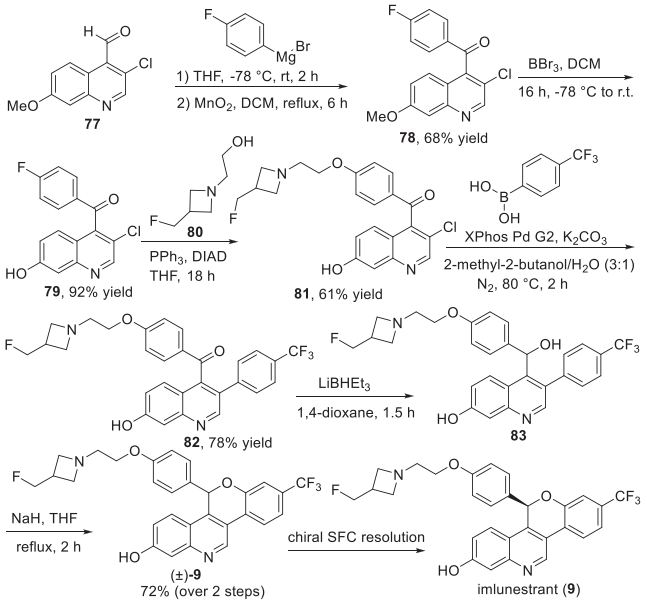
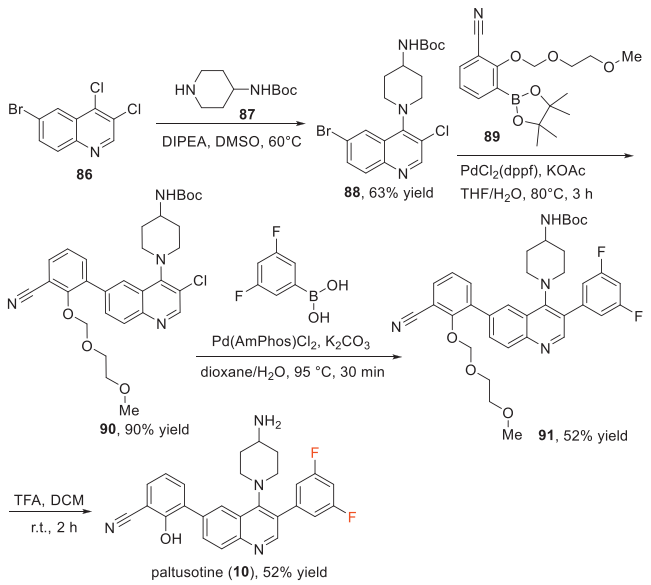


Fig. 5. Structure of imlunestrant (**9**) and its non-trifluoromethylated analog (**76**).



Scheme 10. Synthesis of imlunestrant (**9**).



Scheme 11. Synthesis of paltusotine (**10**).

chromatography (SFC) resolution afforded the enantiopure product imlunestrant (**9**) [106].

11. Paltusotine (Palsonify)

Paltusotine (**10**, brand name: Palsonify) is a 4-(4-aminopiperidinyl)-3,6-diarylquinoline derivative manufactured by Crinetics Pharmaceuticals Inc. (San Diego, USA) as a selective orally non-peptide somatostatin receptor subtype 2 (SST_2) agonist for the treatment of acromegaly and neuroendocrine tumors (NETs) [107–109]. Paltusotine (**10**) demonstrated exceptional potency ($hSST_2$ $EC_{50} = 0.25$ nmol/L, $pEC_{50} = 9.6 \pm 0.2$) and >1000-fold selectivity over other somatostatin receptor subtypes (SST_1, SST_3, SST_4, and SST_5), showing significantly greater activity compared to other analogs bearing fluoro and cyano substituents (compound **84**, $EC_{50} = 10$ nmol/L) and to compound **85**, which contains two hydrogens instead of fluorine atoms ($EC_{50} = 1.9 \pm 0.1$ nmol/L) as illustrated in Fig. 6 [107]. Palsonify provides a once-daily oral therapy that effectively suppresses growth hormone (GH) secretion and reduces insulin-like growth factor-1 (IGF-1) levels, thereby maintaining biochemical control in acromegaly patients [108,109]. Following promising clinical results in Phase II studies demonstrating durable GH and IGF-1 suppression in patients switched from injectable somatostatin analogs, the FDA approved Palsonify on September 25, 2025, for the treatment of acromegaly in adults who had an inadequate response to surgery and/or for whom surgery is not an option [110]. This approval marks Palsonify as the first non-peptide SST_2 agonist to reach the market, representing a major advancement in the management of acromegaly through convenient effective oral therapy [107–110].

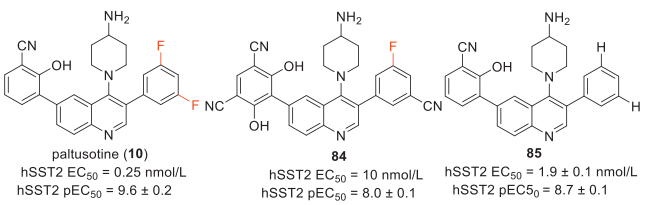


Fig. 6. Structure of paltusotine (**10**) and its monofluorinated and non–fluorinated analogs.

The synthesis of paltusotine (**10**), as depicted in Scheme 11, commenced with 6–bromo–3,4-dichloroquinoline (**86**), which was treated with *tert*–butyl piperidin-4-ylcarbamate (**87**) and DIPEA in DMSO, affording the intermediate **88** in 63 % yield. This intermediate was then subjected to a Suzuki coupling with boronate **89** in the presence of $PdCl_2$(dppf) and KOAc in THF/H_2O at 80 °C to produce the intermediate **90**. This intermediate **90** underwent a second Suzuki coupling with (3,5-difluorophenyl)boronic acid, catalyzed by Pd(AmPhos)Cl_2 and K_2CO_3 in 1,4-dioxane/H_2O to afford the intermediate **91**. Finally, removal of the protecting group under acidic conditions furnished paltusotine (**10**) in 52 % yield [107].

12. Remibrutinib (Rhapsido)

Remibrutinib (**11**, brand name Rhapsido) is a highly selective covalent Bruton's tyrosine kinase (BTK) inhibitor developed by Novartis Pharmaceuticals (Basel, Switzerland) [111]. On September 30, 2025, Rhapsido received its first approval from the FDA for oral use in adult patients with chronic spontaneous urticaria (CSU) who remain symptomatic despite second-generation H1-antihistamine therapy [112]. The incorporation of fluorine into the chemical structure of Remibrutinib (**11**) significantly enhances its pharmacological potency compared to that of the analog **92** (Fig. 7). This modification exhibits superior

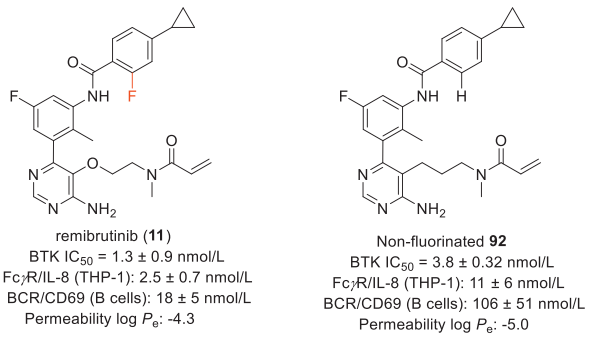
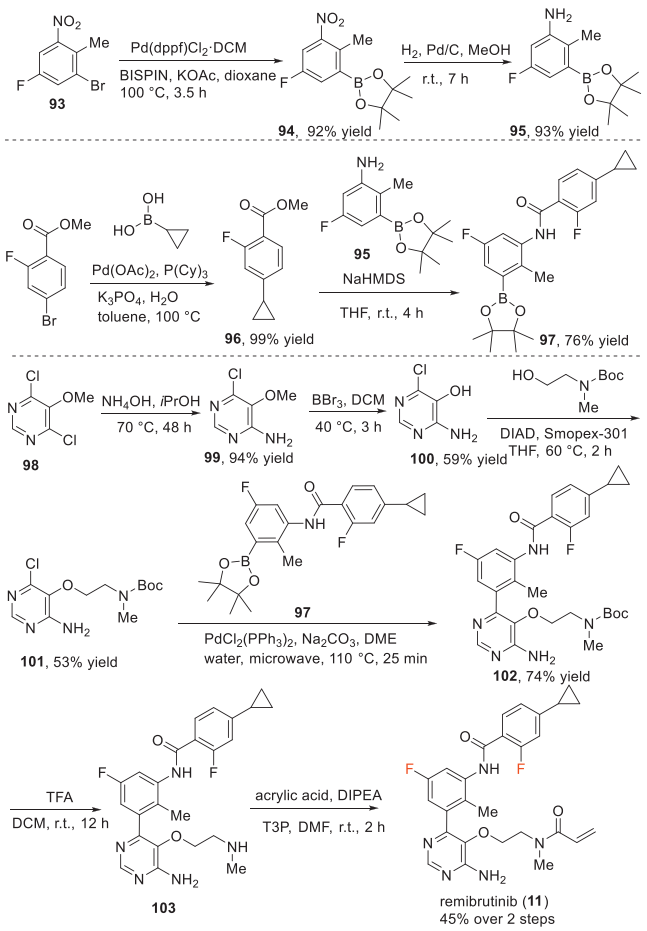


Fig. 7. Structure of remibrutinib (**11**) and its analog **92**.



Scheme 12. Synthesis of remibrutinib (**11**).

BTK inhibition ($IC_{50} = 1.3 \pm 0.9$ nmol/L *vs.* 3.8 ± 0.32 nmol/L). Similar trends are observed across additional pharmacological assays, including FcγR/IL-8 inhibition in THP-1 cells (2.5 ± 0.7 nmol/L *vs.* 11 ± 6 nmol/L) and BCR/CD69 activation in B cells (18 ± 5 nmol/L *vs.* 106 ± 51 nmol/L). Furthermore, fluorination improves membrane permeability ($\log P_e$ −4.3 *vs.* −5.0), thereby increasing cellular absorption [111,113]. In clinical trials, including Phase II and III studies, Remibrutinib showed early and sustained efficacy in CSU patients, with significant reductions in urticaria activity scores (UAS7 = 0 or ≤6) as early as week 1, particularly at the 25 mg twice-daily dose [112,114]. Additionally, remibrutinib (**11**) demonstrated therapeutic potential in other BTK-mediated diseases such as multiple sclerosis, chronic lymphocytic leukemia (CLL), and B-cell malignancies [115]. Thanks to all above information as well as its oral administration and a favorable safety profile, remibrutinib (**11**) represents a promising targeted therapy for patients with moderate to severe CSU and other mast cell-, basophil-, and B-cell-driven disorders [112–114].

The synthetic preparation of remibrutinib (**11**) was shown in Scheme 12. First, borylation of 1–bromo–5-fluoro-2-methyl-3-nitrobenzene using bis(pinacolato)diboron (BISPIN), Pd(dppf)Cl_2, and potassium acetate afforded boronic ester **94**, which was subsequently reduced by catalytic hydrogenation to give aniline **95**. In parallel, Suzuki coupling of methyl 4–bromo–2-fluorobenzoate with cyclopropylboronic acid produced ester **96**, which underwent NaHMDS-mediated amide formation with aniline **95** to give the boronic ester intermediate **97**. The second fragment of the molecule was assembled starting from 2,4-dichloro-3-methoxypyrimidine **98**, which was converted to aminopyrimidine **99** *via* amination, followed by demethylation with boron tribromide to give aminopyrimidinol **100**. Introduction of the linker was achieved through a Mitsunobu reaction with *N*-Boc-*N*-methyl-2-hydroxyethylamine in the presence of DIAD and polymer-supported triphenylphosphine (Smopex-301), forming the intermediate **101**. Next, the Suzuki coupling of intermediates **97** and **101** afforded the Boc-protected intermediate **102**. Finally, Boc deprotection and amide coupling with acrylic acid using propylphosphonic anhydride (T3P) provided the final product remibrutinib (**11**) [111,116].

13. Elinzanetant (Lynkuet)

Elinzanetant (**12**, brand name Lynkuet) is a potent and selective dual neurokinin-1 and neurokinin-3 (NK1/NK3) receptor antagonist developed by Bayer AG (Leverkusen, Germany). On October 24, 2025, it received its first approval from the FDA for the treatment of moderate to severe vasomotor symptoms (VMS) associated with menopause [117]. Elinzanetant (**12**) exerts its therapeutic effect through simultaneous antagonism of NK1 and NK3 receptors ($pK_i = 8.7–10.2$ and 8.0–8.8, respectively; $K_i \approx 0.2–2$ nmol/L), thereby modulating the neurokinin kisspeptin system that regulates thermoregulatory and reproductive hormone signaling [118,119]. Fluorine incorporation into the molecular scaffold enhances receptor binding affinity and stability compared to its analog **104** ($K_i \approx 1–10$ nmol/L) as illustrated in Fig. 8 [119,120]. In Phase II and III trials, Elinzanetant significantly reduced the mean daily frequency of moderate to severe vasomotor episodes by 6.5 episodes at week 4 and 7.8 episodes at week 12 [117,121]. Treatment also improved sleep quality and mood, while serious adverse events were rare (≤2.5 %) [117,120]. Additionally, elinzanetant (**12**) has shown promise in suppressing reproductive hormone levels, including estradiol and luteal-phase progesterone, without inducing vasomotor side effects, suggesting potential utility in hormone-driven conditions such as uterine fibroids and endometriosis [121]. With its non-hormonal mechanism, robust efficacy, and favorable safety profile, Lynkuet represents a novel targeted therapy addressing the unmet need for effective management of menopausal vasomotor symptoms and related endocrine conditions [117–122].

The synthesis of elinzanetant (**12**) was depicted in Scheme 13. It was started with 4–chloro–5-nitropyridin-2(1*H*)-one (**105**), which was subjected to Suzuki coupling with 4-fluoro-2-methylphenylboronic acid in the presence of Pd(dppf)Cl_2 and K_2CO_3 in 1,4-dioxane/H_2O, affording the intermediate **106**. This intermediate was then reacted with $POCl_3$ to produce chlorinated compound **107**. The resulting nitro derivative underwent catalytic hydrogenation using 10 % Pd/C in EtOH under 50 psi H_2 to afford amine **108**. Subsequent amide coupling of amine **108** with acyl chloride **109** afforded the intermediate **110**. *N*-Methylation of resulting **110** with MeI and Cs_2CO_3 in DMF furnished the key intermediate **111**, which was then coupled *via* nucleophilic aromatic substitution (S_NAr) with the upper fragment **112** using DI-

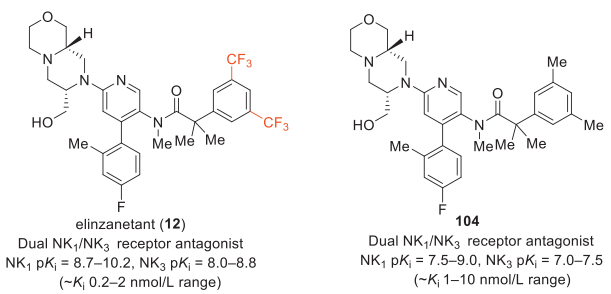
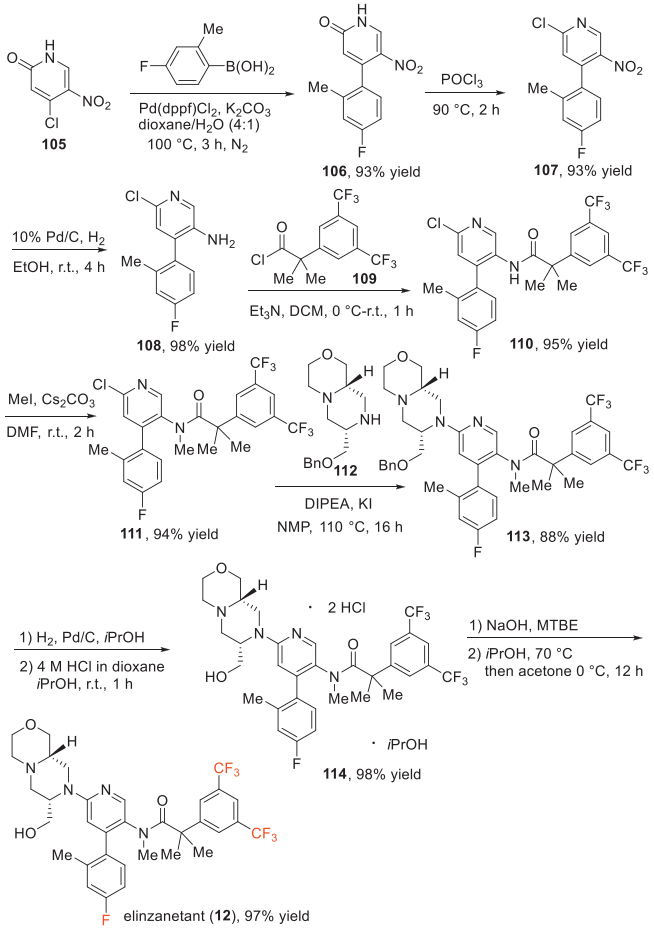


Fig. 8. Structure of elinzanetant (**12**) and its analog **104**.

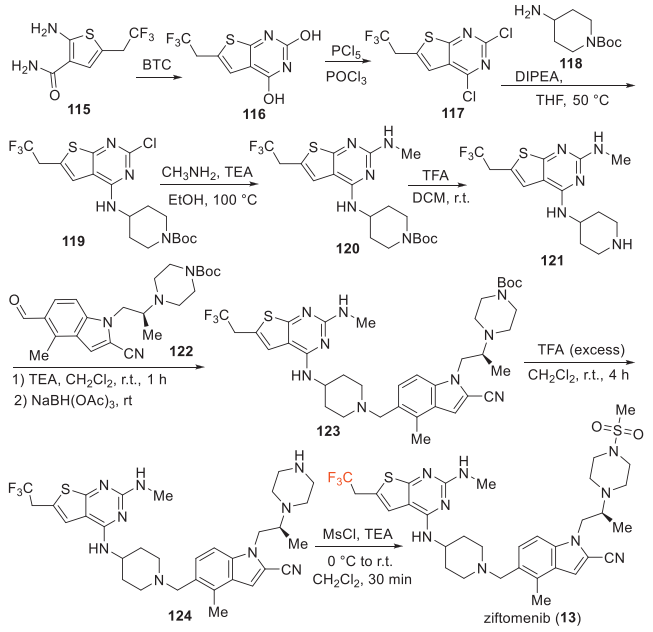


Scheme 13. Synthesis of elinzanetant (**12**).

PEA and KI in *N*-methylpyrrolidone (NMP) to form the intermediate **113**. Salt formation with 4 mol/L HCl in dioxane/isopropanol delivered compound **114**·hydrochloride. Finally, treatment with NaOH followed by crystallization from isopropanol/acetone yielded elinzanetant (**12**) as anhydrous crystalline compound [123].

14. Ziftomenib (Komzifti)

Ziftomenib (**13**, brand name Komzifti) is a potent selective menin inhibitor developed by Kura Oncology (San Diego, California, USA) for the treatment of relapsed or refractory acute myeloid leukemia (AML) driven by nucleophosmin 1 (NPM1) mutations or lysine methyltransferase 2A/mixed lineage leukemia 1 (KMT2A/MLL1) rearrangements. On November 13, 2025, it received its first approval from the FDA for adult patients with relapsed or refractory AML harboring a susceptible NPM1 mutation lacking satisfactory alternative treatment options [124,125]. Ziftomenib showed high biochemical and cellular potency, with an IC_{50} <50 nmol/L with menin and a peptide containing the high affinity menin binding motif found (in MLL in a fluorescence polarization assay) and GI_{50} <10 nmol/L (in MLLAF9 bone marrow cells) [126]. Ziftomenib effectively disrupts the menin–MLL1 protein–protein interaction, a central epigenetic driver sustaining leukemogenic transcriptional programs involving HOX, MEIS1, PBX3, FLT3, and BCL2 [126,127]. In clinical studies, Ziftomenib demonstrated a manageable safety profile with expected hematologic toxicities and differentiation syndrome (15 %). The recommended 600-mg dose achieves complete remission (CR) with partial hematologic recovery (CRh) in 25 % of patients with KMT2A rearrangements or NPM1 mutations, including 35 % CR in the NPM1mut subgroup [127]. Based on promising preclinical data and clinical complete responses, Komzifti represents a major advance in precision epigenetic therapy and has the potential to become the next novel class of targeted therapy in leukemias [124–127].



Scheme 14. Synthesis of ziftomenib (**13**).

The synthetic preparation of ziftomenib (**13**), as outlined in Scheme 14, began with the construction of the thienopyrimidine core. Treatment of 2-amino-5-(2,2,2-trifluoroethyl)thiophene-3-carboxamide (**115**) with bis(trichloromethyl) carbonate (BTC) furnished the key bicyclic intermediate **116**. Subsequent chlorination using a combination of PCl_5 and $POCl_3$ produced compound **117**, which then underwent nucleophilic substitution with *tert*–butyl 4-aminopiperidine-1-carboxylate **118** in the presence of DIPEA to afford the mono-substituted chloride intermediate **119**. A second substitution with methylamine in heated EtOH provided compound **120**, followed by Boc deprotection with trifluoroacetic acid to form the corresponding diamine fragment **121**. Next, the resulting fragment underwent reductive amination with (*S*)-indole derivative **122** in the presence of TEA and $NaBH(OAc)_3$ to afford protected the indole–piperazine conjugate **123**, which was subsequently subjected to Boc-removal using excess of TFA to furnish free indole–piperazine amine **124**. Finally, mesylation with mesyl chloride (MsCl) and TEA provided ziftomenib (**13**) [128,129].

15. Zoliflodacin (Nuzolvence)

Zoliflodacin (**14**, brand name Nuzolvence) is a novel oral antibiotic that was approved by the FDA in December 2025 for the treatment of uncomplicated genitourinary gonorrhea infections in adults and adolescents aged 12 years or older (weighing ≥35 kg) [130,131]. It has a unique mechanism of action and is effective against multidrug-resistant strains. Zoliflodacin (**14**) is a first-in-class oral antibiotic belonging to the spiropyrimidinetrione class [132]. It exerted bactericidal effects by inhibiting the DNA replication of Neisseria gonorrhoeae, specifically through targeting a particular subunit of bacterial topoisomerase IV [133,134]. Its unique mechanism of action ensured no cross-resistance with existing antibiotics such as fluoroquinolones, and it remained active against multidrug-resistant strains, including those resistant to ceftriaxone and azithromycin.

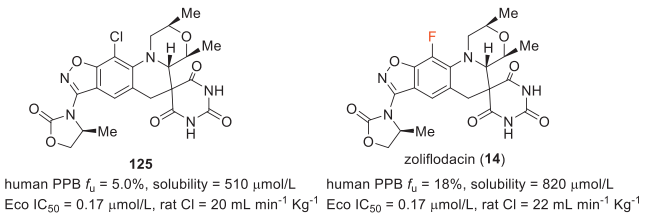
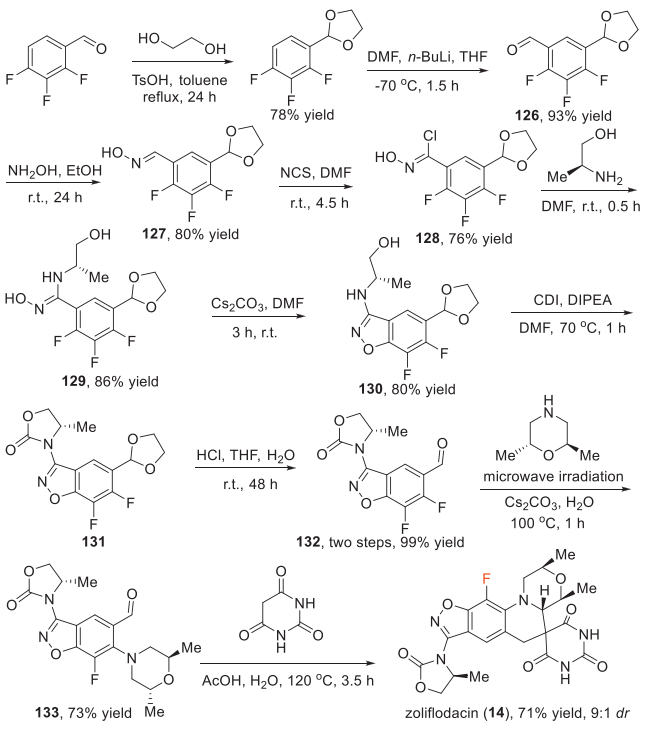


Fig. 9. Structure of zoliflodacin (**14**) and its analog **125**.

The SAR studies showed that the analog of zoliflodacin (**14**) with chloro on the benzo[*d*]isoxazole unit featured a decreased human plasma protein binding (PPB) f_u value and a lower solubility (510 μmol/L). Although a similar *Escherichia coli* FP-based DNA gyrase inhibitory activity was obtained, distilling f_u, antibacterial activity, and rat clearance (Cl) disclosed that zoliflodacin (**14**) was a more favorable compound (Fig. 9). Compared with its analogs, zoliflodacin (**14**) showed virtually no evidence of genotoxicity at the highest concentrations tested in both mouse micronucleus chromosome aberration assay (MMA) and mouse lymphoma assay (MLA). Also, the mammalian cellular toxicity studies disclosed that zoliflodacin (**14**) showed no activity against myeloid and erythroid cell lines at the highest concentration tested of 100 μmol/L. Moreover, zoliflodacin (**14**) demonstrated efficacy in a *S. aureus* neutropenic thigh infection model in mice. It showed a static response at about 10 mg kg^{-1} d^{-1}. Maximal responses of nearly a 2-log reduction in CFU were seen at 25 and 50 mg kg^{-1} d^{-1}. Based on these results, zoliflodacin (**14**) was selected for preclinical development [132].

The synthesis of zoliflodacin (**14**) was shown in Scheme 15 [132], which involved the key steps of constructing benzisoxazole, oxazolidinone, and chiral fused morpholine cyclic unit. First, the protection of 2,3,4-trifluorobenzaldehyde by glycol resulted in the corresponding acetal in 78% yield, which underwent a fluorine-directed *ortho*-lithiation followed by treatment with DMF to form



Scheme 15. Synthesis of zoliflodacin (**14**).

the aldehyde intermediate **126**. Subsequently, aldehyde **126** was converted into oxime **127**, which was further treated with *N*-chlorosuccinimide (NCS), yielding oximoyl chloride **128**. Then, chloride displacement of oximoyl chloride **128** by (*S*)-2-aminopropan-1-ol to give the intermediate **129**. Cyclization of the intermediate **129** in the presence of an inorganic base afforded the benzisoxazole intermediate **130** in 80% yield. The second cyclization reaction of aminoalcohol **130** with CDI furnished the oxazolidinone **131**, which underwent the hydrolysis of the acetal group affording aldehyde intermediate **132**. The fluoride adjacent to the aldehyde group in compound **132** was displaced by chiral dimethylmorpholine *via* a S_NAr reaction furnishing the intermediate 1**33**, which underwent a Knövenagel condensation with pyrimidine-2,4,6(1*H*,3*H*,5*H*)-trione in the presence of acetic acid followed by a tertiary amino effect reaction affording the desired zoliflodacin (**14**) with 9:1 distereoselectivity. The major isomer zoliflodacin (**14**) could be separated from the minor diastereomers.

16. Conclusions and outlook

The fourteen newly approved fluorine-containing drugs discussed in this article display wide-ranging structural diversity, chemical functionality, and therapeutic applications. Yet they share notable common features: All but three contain heterocyclic moieties, and most are chiral compounds, reflecting the dominance of heterocycles in drug scaffolds and the growing emphasis on enantiopure development. Fluorination patterns also follow established medicinal chemistry strategies. Aromatic mono–fluorination is observed in compounds **1**, **3**, **4A**, **5**, **6**, **7**, **8**, **11**, **12**, and **14**; difluorination in **2**, **3**, and **10**; aromatic trifluoromethyl (CF_3) substitution in **4B**, **9**, and **12**; and aliphatic fluorination in **2**, **9**, and **13**. This distribution mirrors trends seen in previous years, underscoring the enduring role of fluorine in fine–tuning drug properties. Aromatic fluorination remains the most common approach, as it subtly modulates electron density and metabolic stability without adding steric bulk, while CF_3 groups and difluorination enhance lipophilicity and block metabolic "hot spots". Aliphatic fluorination, though less frequent, stabilizes C–H bonds and influences conformational preferences. Together, these recurring motifs highlight how heterocycles, chirality, and fluorine substitution continue to serve as reliable design principles for optimizing potency, selectivity, and pharmacokinetics in modern drug development.

Fluorine scanning and structural editing have become indispensable strategies in contemporary medicinal chemistry, exerting a profound influence on the broader field of organic synthesis. By systematically exploring fluorine substitution, researchers can fine–tune molecular properties such as potency, selectivity, metabolic stability, and pharmacokinetics. This methodological integration has transformed drug discovery pipelines, making fluorination not merely a tactical modification but a central design principle.

It should be noted that the introduction of fluorine atoms may also lead to increased potential toxicity due to enhanced metabolic stability. Moreover, enzymatic metabolism of the active agent may lead to a loss of fluorination and the formation of metabolites that could probably affect the safety of therapy. Consequently, the prevalence of fluorinated pharmaceuticals on the global market is projected to continue its steady expansion in the coming years, reflecting both the proven success of fluorine chemistry and its enduring role in shaping next–generation therapeutics.

There are still great challenges and good opportunities in the design and development of fluorine-containing drugs in the future. These include developing greener and more efficient fluorination synthetic methods, exploring new fluorination patterns, utilizing artificial intelligence to assist in predicting the fluorine atom sites in the optimization of lead compounds, and assessing the

persistence and degradation of fluorine-containing drugs in the environment.

CRediT authorship contribution statement

Qian Wang: Writing – original draft, Software, Methodology. **Yeping Bian:** Writing – review & editing, Writing – original draft, Methodology, Investigation, Formal analysis, Conceptualization. **Elias Abouchabaka:** Writing – original draft, Software, Methodology, Data curation. **Daniel Baecker:** Writing – review & editing, Writing – original draft, Validation, Supervision, Project administration, Methodology, Investigation, Formal analysis, Conceptualization. **Gagan Dhawan:** Writing – original draft, Validation, Methodology, Formal analysis. **Anas Semghouli:** Writing – original draft, Software, Methodology, Formal analysis. **Loránd Kiss:** Writing – review & editing, Writing – original draft, Validation, Supervision, Project administration, Methodology, Investigation, Formal analysis, Conceptualization. **Wei Zhang:** Writing – review & editing, Writing – original draft, Supervision, Methodology, Investigation, Formal analysis, Conceptualization. **Vadim A. Soloshonok:** Writing – review & editing, Writing – original draft, Supervision, Project administration, Investigation, Formal analysis, Data curation, Conceptualization. **Jianlin Han:** Writing – review & editing, Writing – original draft, Supervision, Project administration, Methodology, Investigation, Formal analysis, Conceptualization.

Declaration of competing interest

The authors declare that they have no known competing financial interests or personal relationships that could have appeared to influence the work reported in this paper.

Acknowledgments

We gratefully acknowledge the financial support from the National Natural Science Foundation of China (No. 21761132021), the Qing-Lan Project of Jiangsu Province (for Han), the National Research, Development and Innovation Office of Hungary (No. NKFIH/OTKA K 142266), and IKERBASQUE, Basque Foundation for Science (for Soloshonok). The publication of this article was funded by Freie Universität Berlin.

References

[1] G. Chandra, D.V. Singh, G.K. Mahato, S. Patel, Chem. Pap. 77 (2023) 4085–4106.
[2] D. O'Hagan, R.J. Young, Med. Chem. Res. 32 (2023) 1231–1234.
[3] V.A. Soloshonok, K. Mikami, T. Yamazaki, J.T. Welch, Current Fluoroorganic Chemistry: New Synthetic Directions, Technologies, Materials, and Biological Application, J.F. Honek (Ed.), Oxford University Press, 2007 ACS Symposium Series #949.
[4] J. Wang, M. Sánchez-Roselló, J.L. Aceña, et al., Chem. Rev. 114 (2014) 2432–2506.
[5] Y. Zhou, J. Wang, Z. Gu, et al., Chem. Rev. 116 (2016) 422–518.
[6] J. Han, L. Kiss, H. Mei, et al., Chem. Rev. 121 (2021) 4678–4742.
[7] S.V. Kobzev, V.A. Soloshonok, S.V. Galushko, Y.L. Yagupolskii, V.P. Kukhar, Zh. Obshch. Khim. 59 (1989) 909–912.
[8] E.P. Gillis, K.J. Eastman, M.D. Hill, D.J. Donnelly, N.A. Meanwell, J. Med. Chem. 58 (2015) 8315–8359.
[9] Q. Wang, Y. Bian, G. Dhawan, et al., Chin. Chem. Lett. 35 (2024) 109780.
[10] J. Han, A. Wzorek, T. Ono, K.D. Klika, V.A. Soloshonok, Ukr. Chem. J. 91 (2025) 15–54.
[11] J. Han, A. Wzorek, G. Dhawan, et al., Ukr. Chem. J. 90 (2024) 31–56.
[12] J. Han, A. Wzorek, G. Dhawan, et al., Ukr. Bioorg. Acta 19 (2024) 3–20.
[13] N. Wang, H. Mei, G. Dhawan, et al., Molecules 28 (2023) 3651.
[14] Q. Wang, J. Han, A. Sorochinsky, et al., Pharmaceuticals 15 (2022) 999.
[15] A. Liu, J. Han, A. Nakano, et al., Chirality 34 (2022) 86–103.
[16] H.A. Blair, Drugs 85 (2025) 965–975.
[17] Y. Lei, M. Zheng, P. Chen, et al., ChemMedChem 20 (2025) e202500262.
[18] V. Di Lauro, A. Rizzo, M. Tafuro, et al., Cancer Treat. Rev. 140 (2025) 103023.
[19] L. Marzi, K. Agama, J. Murai, et al., Mol. Cancer Ther. 17 (2018) 1694–1704.
[20] H. Ma, B. Chen, Y. Wanf, et al., Chem. Biodivers. 17 (2020) e2000068.
[21] M. Zhang, L.Z. Zhu, C.J. Yang, et al., Bioorg. Chem. 139 (2023) 106652.
[22] V. Alla, R. Rao, C. Ramarao, et al., Patent, WO2012032531A1, 2012.
[23] A.C. Flick, C.A. Leverett, H.X. Ding, et al., J. Med. Chem. 64 (2021) 3604–3657.
[24] S.J. Keam, Drugs 85 (2025) 845–851.
[25] M. Jones, A. Demery, R.A. Al-Horani, Drugs Drug Candidates 4 (2025) 32.
[26] E.B. Cho, C. Jiang, Z. Wang, et al., Trends Pharmacol. Sci. 46 (2025) 480–481.
[27] Z. Wu, D. Lu, Eur. J. Med. Chem. 302 (2026) 118326.
[28] J.N. Wood, N. Yan, J. Huang, et al., J. Gen. Physiol. 157 (2025) e202513778.
[29] C. Harrison, Patent, WO2022256660A1, 2022.
[30] S.M. Hoy, Drugs 85 (2025) 977–984.
[31] G. Oztosun, A. Armstrong, A.C. Hirbe, Expert Opin. Investig. Drugs 34 (2025) 665–673.
[32] I. Hyohdoh, N. Furuichi, T. Aoki, et al., ACS Med. Chem. Lett. 4 (2013) 1059–1063.
[33] T. Ram, A.K. Singh, A. Kumar, et al., RSC Med. Chem. 14 (2023) 1837–1857.
[34] Q. Dong, D.R. Dougan, X. Gong, et al., Bioorg. Med. Chem. Lett. 21 (2011) 1315–1319.
[35] J. Zeng, Z. Luo, T. Zhao, et al., Chem. Biol. Drug Des. 105 (2025) e70067.
[36] C. Hao, X. Li, Z. Wang, et al., Eur. J. Med. Chem. 251 (2023) 115236.
[37] H.A. Blair, Drugs 85 (2025) 1319–1327.
[38] N. Ishii, N. Harada, E.W. Joseph, et al., Cancer Res. 73 (2013) 4050–4060.
[39] A.A. Al-Karmalaway, M.E. Eissa, N.A. Ashour, et al., RSC Adv. 15 (2025) 36441–36471.
[40] M. Murakata, T. Ikeda, T. Ichige, Patent, EP2754654A1, 2012.
[41] C. Zhang, Y. Rao, ACS Med. Chem. Lett. 16 (2025) 907–910.
[42] S. Wang, R.H. Zhang, H. Zhang, et al., Eur. J. Med. Chem. 222 (2021) 113573.
[43] Y. Su, R. Li, X. Ning, et al., Eur. J. Med. Chem. 177 (2019) 32–46.
[44] C. Brullo, B. Tasso, Curr. Med. Chem. 28 (2021) 3318–3338.
[45] C. Guo, Q. Li, J. Xiao, et al., J. Biomol. Struct. Dyn. 41 (2023) 8654–8670.
[46] M.J. Luzzio, K.D. Freeman-Cook, S.K. Bhattacharya, et al., Patent, US2009054395A1, 2008.
[47] M. Pérol, N. Yang, C.M. Choi, et al., Ann. Oncol. 34 (2023) S788–S789.
[48] G. Harada, F.C. Santini, C. Wilhelm, A. Drilon, Lung Cancer 161 (2021) 108–113.
[49] W. Li, A. Xiong, N. Yang, et al., J. Clin. Oncol. 42 (2024) 2660–2670.
[50] M. Nagasaka, D. Brazel, S.I. Ou, Expert Opin. Investig. Drugs 33 (2024) 79–84.
[51] S. Waliany, J.J. Lin, Lung Cancer J. Clin. Oncol. 42 (2024) 2622–2627.
[52] M. Nagasaka, Y. Ohe, C. Zhou, et al., Future Oncol. 19 (2023) 123–135.
[53] T. Yasuyuki, Y. Kenji, K. Yoshiko, et al., Patent, US 2015051190A1, 2015.
[54] M.H. Sheridan, Drugs 86 (2026) 249–257.
[55] F. Zhou, D.D. Chen, F. Guo, Patent, WO2023220967A1, 2023.
[56] Y. Takeda, K. Yoshikawa, Y. Kagoshima, Patent, WO2013183578A1, 2013.
[57] S. Vyse, P.H. Huang, Signal Transduct. Target Ther. 4 (2019) 5.
[58] J.R. Molina, P. Yang, S.D. Cassivi, S.E. Schild, A.A. Adjei, Mayo. Clin. Proc. 83 (2008) 584–594.
[59] S. Novello, F. Barlesi, R. Califano, et al., Ann. Oncol. 27 (5) (2016) v1–v27 suppl.
[60] M. Maemondo, A. Inoue, K. Kobayashi, et al., N. Engl. J. Med. 362 (2010) 2380–2388.
[61] R. Rosell, E. Carcereny, R. Gervais, et al., Lancet Oncol. 13 (2012) 239–246.
[62] Y.L. Wu, C. Zhou, C.P. Hu, et al., Lancet Oncol. 15 (2014) 213–222.
[63] J.D. Moyer, E.G. Barbacci, K.K. Iwata, et al., Cancer Res. 57 (1997) 4838–4848.
[64] M.E. Arcila, K. Nafa, J.E. Chaft, et al., Mol. Cancer Ther. 12 (2013) 220–229.
[65] M. Wang, Y. Xu, W.T. Huang, et al., Lung Cancer 199 (2025) 108053.
[66] D. Seo, J.H. Lim, Int. J. Mol. Sci. 25 (2024) 5917.
[67] J. Wang, D. Lam, J. Yang, L. Hu, Med. Chem. Res. 31 (2022) 1647–1662.
[68] O. Illini, F.C. Saalfeld, P. Christopoulos, et al., Int. J. Mol. Sci. 25 (2024) 3992.
[69] S. Vyse, P.H. Huang, Expert Rev. Anticancer Ther. 22 (2022) 3–16.
[70] S. Dhillon, Drugs 83 (2023) 1629–1634.
[71] K. Sangwan, G. Agarwal, Invest. New Drug 43 (2025) 1177–1189.
[72] T. Mitsudomi, Transl. Lung Cancer Res. 14 (2025) 334–340.
[73] M. Wang, J.C. Yang, P.L. Mitchell, et al., Cancer Discov. 12 (2022) 1676–1689.
[74] Y.T. Wang, P.C. Yang, J.Y. Zhang, J.F. Sun, Molecules 29 (2024) 1448.
[75] Z. Li, H. Zou, W. Zhu, et al., Patent, WO2019149164A1, 2019.
[76] S. De Maat, Z.L.M. Hofman, C. Maas, J. Thromb. Haemost. 16 (2018) 1674–1685.
[77] P.J. Busse, S.C. Christiansen, N. Engl. J. Med. 382 (2020) 1136–1148.
[78] P.J. Busse, S.C. Christiansen, M.A. Riedl, J Allergy Clin. Immunol. Pract. 9 (2021) 132–150.
[79] S.D. Betschel, A. Banerji, P.J. Busse, D.M. Cohn, M. Magerl, J. Allergy Clin. Immunol. Pract. 11 (2023) 2315–2325.
[80] T. Do, M.A. Riedl, Immunol. Allergy Clin. North. Am. 44 (2024) 561–576.
[81] T.D. Smith, M.A. Riedl, Ann. Allergy Asthma Immunol. 133 (2024) 380–390.
[82] H.J. Longhurst, M. Cancian, V. Grivcheva-Panovska, et al., Clin. Rev. Allergy Immunol. 67 (2024) 83–95.
[83] M.A. Riedl, E. Aygören-Pürsün, J. Baker, Allergy 73 (2018) 1871–1880.
[84] P.L. Kotian, M. Wu, S. Vadlakonda, et al., J. Med. Chem. 64 (2021) 12453–12468.
[85] A. McDonald, S. Qian, I. Kalfus, Patent, WO2019/166874, 2019.
[86] I. Kalfus, A. McDonald, S. Qian, J. Allergy Clin. Immunol. 139 (2017) AB378.
[87] M.A. Riedl, H. Farkas, E. Aygören-Pürsün, et al., N. Engl. J. Med. 391 (2024) 32–43.
[88] R.L. Davie, H.J. Edwards, D.M. Evans, et al., J. Med. Chem. 65 (2022) 13629–13644.
[89] N. Cooper, W. Ghanima, N. Engl. J. Med. 381 (2019) 945–955.
[90] F. Rodeghiero, R. Stasi, T. Gernsheimer, et al., Blood 113 (2009) 2386–2393.
[91] D.J. Kuter, M. Efraim, J. Mayer, et al., N. Engl. J. Med. 386 (2022) 1421–1431.

[92] G. López-Herrera, A. Vargas-Hernández, M.E. González-Serrano, J. Leukoc. Biol. 95 (2014) 243–250.
[93] L.J. Crofford, L.E. Nyhoff, J.H. Sheehan, P.L. Kendall, Expert Rev. Clin. Immunol. 12 (2016) 763–773.
[94] J. Liu, C. Chen, D. Wang, J. Zhang, T. Zhang, Eur. J. Med. Chem. 217 (2021) 113329.
[95] E.D. Deeks, Drugs 77 (2017) 225–236.
[96] S. Peterson, A. Jalil, K. Beard, M. Kakara, S. Sriwastava, Mult. Scler. Relat. Disord. 68 (2022) 104125.
[97] J.M. Bradshaw, J.M. McFarland, V.O. Paavilainen, et al., Nat Chem. Biol. 11 (2015) 525–531.
[98] C.L. Langrish, J.M. Bradshaw, M.R. Francesco, et al., J. Immunol. 206 (2021) 1454–1468.
[99] T.D. Owens, K.A. Brameld, E.J. Verner, J. Med. Chem. 65 (2022) 5300–5316.
[100] D. Wei, J. Guo, F. Zhu, et al., J. Org. Chem. 90 (2025) 15065–15073.
[101] K.L. Jhaveri, P. Neven, M.L. Casalnuovo, et al., N. Engl. J. Med. 392 (2025) 1189–1202.
[102] S.V. Bhagwat, C. Mur, M. Vandekopple, et al., Cancer Res. 85 (2025) 777–790.
[103] K.L. Jhaveri, E. Lim, R. Jeselsohn, et al., J. Clin. Oncol. 42 (2024) 4173–4186.
[104] J.A. Bastian, J.D. Cohen, A. Rubio, D.J. Sall, Patent, US 2020/017516A1, 2020.
[105] S. Sherman, Z.M. Sandusky, D. Russo, et al., JCI Insight 10 (2025) e188051.
[106] J.A. Bastian, J.D. Cohen, A. Rubio, D.J. Sall, J.A. McMahon, Patent, US 2023/0234960A1, 2023.
[107] J. Zhao, S. Wang, S. Markison, S.H. Kim, S. Han, M. Chen, et al., ACS Med. Chem. Lett. 14 (2023) 66–74.
[108] L.E. Wildemberg, C. Fialho, M.R. Gadelha, et al., Best Pract. Res. Clin. Endocrinol. Metab. 38 (2024) 101906.
[109] A. Madan, S. Markison, S.F. Betz, A. Krasner, R. Luo, et al., Pituitary 25 (2022) 328–339.
[110] R. Luo, A. Madan, C.T. Ferrara-Cook, et al., Br. J. Clin. Pharmacol. 91 (2025) 2070–2079.
[111] D. Angst, F. Gessier, P. Janser, et al., J. Med. Chem. 63 (2020) 5102–5118.
[112] M. Metz, A. Giménez-Arnau, M. Hide, et al., N. Engl. J. Med. 392 (2025) 984–994.
[113] M. Kaul, P. End, M. Cabanski, et al., Clin. Transl. Sci. 14 (2021) 1756–1768.
[114] M. Maurer, W. Berger, A. Giménez-Arnau, et al., J. Allergy Clin. Immunol. 150 (2022) 1498–1506.
[115] Q. Zhang, C. Wen, L. Zhao, Y. Wang, Molecules 28 (2023) 8037.
[116] A. Figuccia, L. Lovelle, M. Parmentier, Patent, WO 2024/069507A1, 2024.
[117] F. Cardoso, S. Parke, D.J. Brennan, et al., N. Engl. J. Med. 392 (2025) 510–519.
[118] K. Francke, S. Klein, J. Burke, et al., Clin. Transl. Sci. 18 (2025) e70282.
[119] M. Hager, T. Goldstein, V. Fitz, et al., Expert Opin. Pharmacother. 25 (2024) 783–789.
[120] M. Trower, Patent, US20160339037A1, 2016.
[121] J.A. Simon, R.A. Anderson, E. Ballantyne, et al., Menopause 30 (2023) 239–246.
[122] S. Pawsey, E.G. Mills, E. Ballantyne, et al., J. Clin. Endocrinol. Metab. 106 (2021) e3221–e3234.
[123] M. Schleusner, M. Ghizzoni, R. Lawrence, Patent, WO2021094247A1, 2021.
[124] W. Fiskus, N. Daver, S. Boettcher, et al., Leukemia 36 (2022) 2729–2733.
[125] T. Cierpicki, J. Grembecka, Annu. Rev. Pathol. Mech. Dis. 20 (2025) 275–301.
[126] J. Rausch, M.M. Dzama, N. Dolgikh, et al., Haematologica 108 (2023) 2837.
[127] E.S. Wang, G.C. Issa, H.P. Erba, et al., Lancet Oncol. 25 (2024) 1310–1324.
[128] T. Wu, L. Li, Y. Wang, et al., Patent, WO 2017/161028A1, 2017.
[129] T. Wu, L. Li, P. Ren, Patent, US 11649251B2, 2023.
[130] A. Luckey, M. Balasegaram, L.A. Barbee, et al., Lancet 407 (2026) 147–160.
[131] K.A. Workowski, Lancet 407 (2026) 106–107.
[132] G.S. Basarab, P. Doig, V. Galullo, et al., J. Med. Chem. 58 (2015) 6264–6282.
[133] S.N. Taylor, J. Marrazzo, B.E. Batteiger, et al., N. Engl. J. Med. 379 (2018) 1835–1845.
[134] P.A. Bradford, A.A. Miller, J. O'Donnell, J.P. Mueller, ACS Infect. Dis. 6 (2020) 1332–1345.